Fuzzy Self-Tuning PID-Based Intelligent Control of an Anti-Wave Buoy Data Acquisition Control System

YAOGUANG WEI[1,2], YINGHAO WU[1], XU ZHANG[1], JIAHUI REN[1], AND DONG AN[1,2]

[1]College of Information and Electrical Engineering, China Agricultural University, Beijing 100083, China
[2]Beijing Engineering Technology Research Center of Internet of things in Agriculture, China Agricultural University, Beijing 100083, China

Corresponding author: Dong An (andong@cau.edu.cn)

ABSTRACT In aquaculture, water quality is influenced by excessive feeding, a high breeding density, the species composition and the distribution of algae species. Traditional buoys can only collect water quality data at a fixed depth, and it is impossible to measure the water quality at different depths in the water column. Sea waves are common in the open ocean and influence data acquisition systems via wave forces, which affect the accuracy of data collection. Considering the above problems, a data acquisition control system with automatic lifting is designed. The underwater acquisition system collects water quality data and sends the data to a microcontroller. The microcontroller sends a displacement control signal to a PLC according to the processed data. The PLC automatically develops the corresponding acceleration and deceleration operating curves according to the displacement. A fuzzy PID self-tuning control method is used to accurately control the speed and steering of the stepping motor, and an IIR digital filter is designed to reduce the interference from sea waves. The simulation results show that the stepping motor responds quickly, the speed of the stepping motor is stable, and the data acquisition time is reduced based on the proposed algorithm. Moreover, wave interference is largely mitigated, and the system is generally stable.

INDEX TERMS Data acquisition control system, automatic lifting, anti-wave interference, fuzzy self-tuning PID, IIR digital filter.

I. INTRODUCTION

Oceans cover 71% of the Earth's surface. As the population continues to increase, land resources are becoming increasingly scarce. Therefore, the abundant fish and mineral resources in the ocean have received increased attention. Due to poor awareness regarding environmental protection and rapid industrial development, large volumes of untreated industrial wastewater, domestic waste and agricultural wastewater are being directly dumped into the ocean and causing the quality of the large-scale water environment to deteriorate. Therefore, to mitigate the further deterioration of the marine environment, real-time monitoring of the marine environment is required, especially for the offshore environment. For example, monitoring and analyzing the

The associate editor coordinating the review of this manuscript and approving it for publication was Mou Chen.

water quality of offshore farms in real time can yield the best breeding conditions for aquaculture animals, reduce fishery losses and increase production. Second, the monitoring of the marine environment is conducive to protecting the environment and maintaining an ecological balance [1]. In addition, according to marine environmental data, the trends in ocean water quality can be predicted in advance to avoid related issues and economic losses. Therefore, obtaining accurate and reliable data and accurate forecasts of the marine environment is very important for protecting the environment and human lives [2], [3].

A traditional buoy can only collect water quality data at a certain fixed depth in the water column. Of course, at some depths in the water environment of an underwater vehicle, it is also necessary to measure the water quality conditions such that an underwater robot can independently work underwater. Robots can perform real-time storage of water quality data,

including image information and video information, and help analyze and research the underwater environment and the water quality to make more accurate judgments. However, because underwater communication is restricted, real-time transmission of data is not possible, and only when the robot is retrieved can all of the data be analyzed [4]. Typically, vertical arrays of anchor instruments and sensors are suspended to monitor a water body at set depths. This self-contained monitoring approach has various advantages [5]; however, it is time consuming and labor intensive, data acquisition is limited and lagging, and it is impossible to automatically measure water quality information in the water depth direction. Moreover, due to the complex topographic environments of lakes, bays and coastal areas, algae are distributed to various degrees based on sunlight attenuation at different depths. Specifically, most water bodies are unevenly exposed to sunlight, and a water body can become stratified. Additionally, the water qualities of different water layers can obviously differ. For example, the thermocline, the oxygen layer, and the salt layer have different depth distributions [6]. AH Mohd Akmal Helmi et al. proposed a mobile floating buoy integrated with multiple water quality monitoring sensors to detect water quality parameters in the area and integrated it with Google Maps. The system can display the location information of the buoy on a computer terminal and send instructions and data transmission to the buoy through the global mobile communication system (GSM). Real-time data transmission is realized, which reduces the cost and improves the efficiency. However, this design is applicable to lakes and large breeding bases. Due to large sea waves, the positioning accuracy is seriously affected [7]. Anthony Ethier designed a buoy to detect information such as water quality. The buoy can measure not only water quality data but also wind speed, wind direction, air temperature and humidity, and it can also take pictures, perform cellular code division multiple access (CDMA) data transmission, carry out remote telemetry, and set the sampling frequency. However, the design does not consider water stratification measurement; rather, it only considers a fixed depth of water quality monitoring [8]. Peter Coad and others designed a buoy to detect water quality data and predict the ability of algae to breed through wireless network transmission to the client and the analysis of water quality using artificial neural network training. The buoy is also a means of obtaining depth-measured water quality data, without considering stratification, water quality and design automatic lifting function [9]. Griffo *et al.* [10] designed a sea buoy with impact resistance effect according to the conditions of sea waves, reducing the impact of waves on the water quality sensor and improving the measurement accuracy. In addition, due to the influence of the sea breeze, buoys are influenced by a rocking motion that affects the accuracy of the underwater sensor and, in turn, the accuracy of data collection. Therefore, monitoring the vertical distribution of the water quality in ocean water or surface water is an important prerequisite for studying water quality factors and ecological environments.

This paper designs a data acquisition controller of a buoy, which can use the water level sensor to automatically control the rise and fall of the underwater acquisition system, measure the water quality parameters of different water depths and automatically adjust the position of the monitoring points in the direction of water depth according to changes in the hydrological environment to conduct stratified monitoring of water bodies. In addition, according to the actual hydrological environment of the buoy, a level 3 sea waves random disturbance model is developed to simulate the operation condition of the system under three sea conditions. This paper studies the buoy measuring range rather than limiting it to a fixed point, expands the measuring range, and performs a comprehensive analysis of the layered structure and water quality for people based on a three-dimensional distribution law.

II. MATERIAL AND METHODS

The data acquisition and control system of a buoy is mainly used to select the appropriate water depth for measurements according to the surrounding hydrological environment. This system can accurately control the dive speed and dive distance of an underwater data acquisition system and can collect the water quality data at different depths for vertical monitoring. The variations in water quality parameters provide data and theoretical support for related analyses.

A data acquisition control system can mainly be divided into an underwater acquisition system, a control system, and an actuator. The underwater acquisition system collects the water quality data, which is then sent to the microcontroller in the control system [11]. The microcontroller sends corresponding displacement control signals to the PLC (programmable logic controller) according to the processed data. The PLC independently develops the corresponding acceleration and deceleration running curve according to the magnitude of the displacement. The fuzzy PID (proportion integral derivative) self-tuning control method is used to accurately control the speed steering of the stepping motor. The stepping motor drives the underwater sealed compartment to the next suitable measurement point using a winch and a hinge. In addition, the control system sends the processed water quality data to the monitoring center through the RF transceiver unit/satellite communication module. If a measured value is larger than the threshold set by the controller, the control system sends a warning message to the monitoring center. The monitoring center can also send instructions according to the collected water quality data to alter the strategy employed by the underwater acquisition at different depths based on two measurement methods: manual measurements and automatic measurements.

As shown in Figure 1, the data acquisition control system is divided into three parts: the underwater acquisition system, the underwater control system, and the lifting actuator. A physical picture of the float is shown below.

As shown in the figure above, the buoy body is equipped with beacon lights (1), a sucker antenna (4), a wind
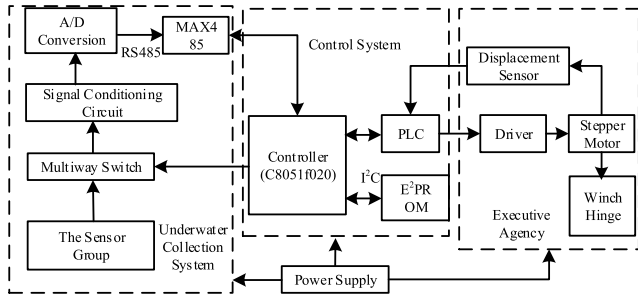
FIGURE 1. Overall structure of the system.

direction and wind speed sensor (5), a wind power generation device (2), and a solar panel (3). The buoy body capsule (10) contains an RF transceiver module/satellite communication module (7), floating data acquisition memory (9), a wind-solar complementary power controller (6), a battery pack (8), and a GPS hall sensor (22). The RF transceiver/satellite communication module (7) is connected to the data acquisition memory (9). The underwater capsule (17) consists of a micro-controller (14), an underwater data acquisition and storage module (12), an underwater sensor group (15), a stepper motor (13), a capstan (18) and a hinge (19) fixed under the underwater capsule. Step motor (13) is connected with a one-way locking switch (11). Through the structure of the buoy block diagram and physical diagram, the underwater acquisition system is located in an underwater sealed compartment and mainly includes sensors, a data acquisition module, and a signal transmission module. The water level sensor, ammonia nitrogen sensor, flow rate detector, and water quality detector (which measures dissolved oxygen, conductivity, temperature, turbidity, and the pH) constitute the sensor group. The data acquisition module mainly includes signal conditioning. The road switch and A/D conversion are involved in the acquisition and conversion of multiparameter analog data [12]. The signal transmission module mainly relies on a communication cable to send the water quality data to the control system.

The water control system is located in the floating body of the buoy and mainly includes a PLC, a data receiving and storage module, a radio frequency transceiver unit/satellite communication module, and a battery pack. The data receiving and storage module adopts E2PROM and is connected to the controller through the I2C bus. This module stores the water quality data sent by the underwater collection system. The controller is controlled by the PLC and connected to the underwater data collection system through the communication cable. The PLC is involved in data collection and storage, and it calls a fuzzy control program to automatically control the running speed, time, and lifting distance of the lifting actuator. In addition, the PLC controls the switching of the power supply mode (battery/solar energy).

The lifting actuators mainly include stepping motors, drives, reducers, position feedback devices (photoelectric encoders), one-way locking switches, winches, and hinges. The stepping motor, drive, reducer, and position feedback
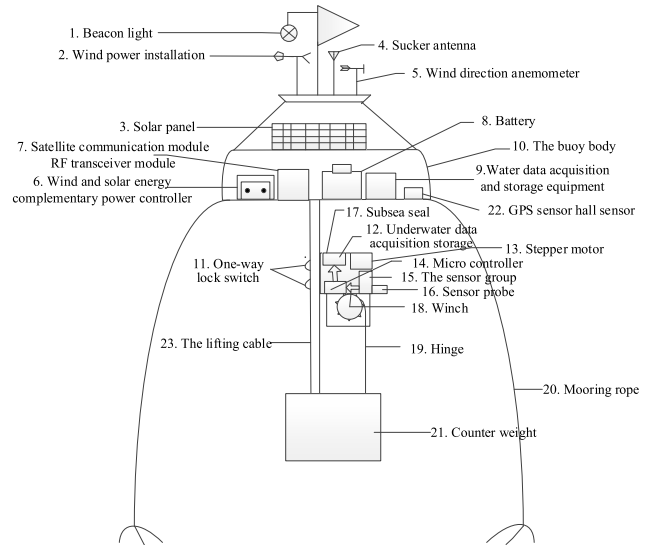

FIGURE 2. Floating buoy physical figure.

device (photoelectric encoder) are located in the floating body; the winch is located under the floating body; one end of the hinge is attached to the winch; and the other end of the hinge is fixed in the underwater sealed compartment, which is one-way locking. The switch connects the underwater sealed compartment with the lifting communication cable.

III. CALCULATION

The water control system of the stepping motor controls the rotation direction and rotation speed of the stepping motor through the driver, and the stepping motor drives the winch, which rotates via a speed reducer so that the underwater sealing compartment moves along the lifting communication cable to accurately reach the designated position. However, when the start frequency of the motor is too high or the load is too large, a step-out phenomenon can occur. In such cases, the starting frequency is much smaller than the maximum operating frequency; when the speed is too high, overtravel, shock, and oscillation issues are likely to occur. Therefore, to ensure the smooth operation of the system, an acceleration and deceleration control method that is simple and can meet the accuracy requirements of practical applications in real time is required for the stepping motor.

Two-phase stepping motor voltage and rotor torque balance equations can be established as follows [13], [14]:

$$U = RI + \rho LI + \rho\theta \frac{\partial}{\partial\theta}LI \qquad (1)$$

$$J\frac{d^2\theta}{dt^2} = T_E - D\frac{d\theta}{dt} - T_L \qquad (2)$$

$$T_E = \frac{1}{2}\sum\frac{\partial Ljj}{\partial\theta}i_j^2 + \frac{1}{2}\sum\frac{\partial L_{jk}}{\partial\theta}i_ji_k$$
$$(j = a, b; k = a, b; j \neq k) \qquad (3)$$

where J is the total inertia of the rotor and load of the motor, T_E is the electromagnetic torque, T_L is the load torque, and D is the viscous friction coefficient. The subvectors and

submatrices are as follows.

$$U = \begin{bmatrix} u_a \\ u_b \end{bmatrix}, \quad R = \begin{bmatrix} R_a & 0 \\ 0 & R_b \end{bmatrix},$$

$$I = \begin{bmatrix} i_a \\ i_b \end{bmatrix}, \quad L = \begin{bmatrix} L_{aa} & L_{ab} \\ L_{ba} & L_{bb} \end{bmatrix}$$

The motor voltage equation with input type (1) is as follows:

$$U = \begin{bmatrix} R_a & 0 \\ 0 & R_b \end{bmatrix} \begin{bmatrix} i_a \\ i_b \end{bmatrix} + \begin{bmatrix} L_{aa} & L_{ab} \\ L_{ba} & L_{bb} \end{bmatrix} \begin{bmatrix} \frac{d\,i_a}{dt} \\ \frac{d\,i_b}{dt} \end{bmatrix}$$
$$+ \frac{d\theta}{dt} \frac{\partial}{\partial \theta} \begin{bmatrix} L_{aa} & L_{ab} \\ L_{ba} & L_{bb} \end{bmatrix} \begin{bmatrix} i_a \\ i_b \end{bmatrix} \quad (4)$$

where u_a, i_a, and R_a are the phase winding voltage, current and resistance of the motor stator a; u_b, i_b, and R_b are the phase winding voltage, current and resistance of motor stator b; and L_{aa}, L_{bb}, L_{ab}, and L_{ba} are the winding self-inductance and mutual inductance variables for stators a and b.

Assuming that the motor is a single-phase excitation motor, the equation of motion for the stepping motor can be obtained as follows:

$$J\frac{d^2\theta}{dt^2} + D\frac{d\theta}{dt} + \frac{1}{2}Z_r Li_a^2 \sin Z_r\theta + T_L = 0 \quad (5)$$

According to (9), we obtain the following equation:

$$J\frac{d^2\theta_1}{dt^2} + D\frac{d\theta_1}{dt} + \frac{1}{2}Z_r Li_a^2 \sin Z_r\theta_1 + T_L$$
$$= J\frac{d^2\theta_0}{dt^2} + D\frac{d\theta_0}{dt} + \frac{1}{2}Z_r Li_a^2 \sin Z_r\theta_0 + T_L \quad (6)$$

When the rotor reaches an equilibrium position, the difference between the actual operating angle and the ideal motor rotation angle is small, that is, $\delta\theta = \theta_1 - \theta_0$ approaches 0, and $\sin Z_r\delta\theta \approx Z_r\delta\theta$. Therefore, equation (6) can be transformed to equation (7).

$$J\frac{d^2(\delta\theta)}{dt^2} + D\frac{d(\delta\theta)}{dt} + \frac{1}{2}Z_r^2 Li_a^2(\delta\theta) = 0 \quad (7)$$

By performing a Lagrangian transformation of equation (7), the stepping motor transfer function G1(s) is as follows.

$$G_1(s) = \frac{Z_r^2 Li_a^2/2J}{s^2 + Ds/J + Z_r^2 Li_a^2/2J} \quad (8)$$

IV. RESULTS
A. FUZZY SELF-TUNING PID SIMULATION
Currently, the conventional PID regulator is widely used in the electromechanical control process because of its simple algorithm. By adjusting the three parameters (KP, KI and KD) of the PID controller, the system achieves the best control effect. Among them, the proportional action controls the adjustment strength of the system; the integral action plays the role of eliminating the error, but the reaction is slow; the differential action plays the role of early control, and the reaction can be eliminated before the error has occurred [15].

To accurately control the system and improve the stability and dynamic response of the system, fuzzy control technology has been combined with classic PID technology, and the error between the actual control effect and the expected control effect and the error rate are used as inputs to the fuzzy control technology. After fuzzy reasoning, the online real-time adjustment of the three PID parameters of the PID occurs.

1) FUZZY LINGUISTIC VARIABLES AND MEMBERSHIP FUNCTIONS
The fuzzy self-tuning PID controller of the system takes the water level deviation E and the rate of change in the water level deviation EC as the input quantities and adjusts the PID parameters in real time using the corresponding fuzzy control rules to determine the fuzzy control outputs as K'$_P$, K'$_I$, K'$_D$. Therefore, the PID parameters are optimized for the different states of the system.

The water level deviation E is $(-3, 3)$, the basic domain is $(-15 \text{ m}, 15 \text{ m})$, the quantization factor is $3/15 = 0.2$, and the membership function is triangular, is divided into 7 levels. The PB-water level parameter deviation is positive, the PM-water level parameter deviation is positive, the PS-water level parameter deviation is small, the ZO-water level parameter deviation is zero, the NS-water level parameter deviation is negative, the NM-water level parameter deviation is negative, and the NB-water level parameter deviation is negative.

The water depth deviation EC is $(-3, 3)$, the basic domain is $(-0.05 \text{ m/s}, 0.05 \text{ m/s})$, the quantization factor is $3/0.05 = 60$, and the membership function is triangular and divided into 7 levels. The rate of change in the PB-water level parameter deviation is positively extreme, the rate of change in the PM-water level parameter deviation is positive, the rate of change in the PS-water level parameter deviation is very small, the rate of change in the ZO-water level parameter deviation is zero, the rate of change in the NS-water level parameter deviation is extremely negative, the rate of change in the NM-water level parameter deviation is moderately negative, and the rate of change in the NB-water level parameter deviation is negative.

The domains of K'P, K'I and K'D are all $(0, 3)$ and divided into 7 levels. The PB parameter adjustment is positive, PM parameter adjustment is moderate, PS parameter adjustment in the forward direction is extremely small, the ZO parameter is adjusted to zero, the NS parameter adjustment is extremely negative, the NM parameter adjustment is moderately negative, and the NB parameter adjustment is extremely negative.

2) CONTROL RULES
The fuzzy self-tuning PID control rules are based on the following principles.

(1) When the absolute value of the water level deviation is sufficiently large, the value of K'$_P$ should be larger, and the value of K'$_D$ should be small to avoid issues caused by the sudden change in the initial absolute value of the water

TABLE 1. K'$_P$ control rules.

EC	E						
	NB	NM	NS	ZO	PS	PM	PB
NB	PB	PB	PM	PM	PS	PS	ZO
NM	PB	PB	PM	PM	PS	ZO	ZO
NS	PM	PM	PM	PS	ZO	NS	NM
ZO	PM	PS	PS	ZO	NS	NM	NM
PS	PS	PS	ZO	NS	NS	NM	NM
PM	ZO	ZO	NS	NM	NM	NM	NB
PB	ZO	NS	NS	NM	NM	NB	NB

TABLE 2. K'$_I$ control rules.

EC	E						
	NB	NM	NS	ZO	PS	PM	PB
NB	NB	NB	NB	NM	NM	ZO	ZO
NM	NB	NB	NM	NM	NS	ZO	ZO
NS	NM	NM	NS	NS	ZO	PS	PS
ZO	NM	NS	NS	ZO	PS	PS	PM
PS	NS	NS	ZO	PS	PS	PM	PM
PM	ZO	ZO	PS	PM	PM	PB	PB
PB	ZO	ZO	PS	PM	PB	PB	PB

TABLE 3. K'$_D$ control rules.

EC	E						
	NB	NM	NS	ZO	PS	PM	PB
NB	PS	PS	ZO	ZO	ZO	PB	PB
NM	NS	NS	NS	NS	ZO	NS	PM
NS	NB	NB	NM	NS	ZO	PS	PM
ZO	NB	NM	NM	NS	ZO	PS	PM
PS	NB	NM	NS	NS	ZO	PS	PS
PM	NM	NS	NS	NS	ZO	PS	PS
PB	PS	ZO	ZO	ZO	ZO	PB	PB

level deviation. In addition, the value of K'$_I$ should be as small as possible, which can reduce the response time and system overshoot.

(2) When the absolute value of the water level deviation is moderate, the value of K'$_P$ should be small to reduce system overshoot; in addition, moderate K'$_I$ and K'$_D$ values should be established to reduce the response of the system.

(3) When the absolute value of the water level deviation is small, the system adjusts the force strain to be small, so the value of K'$_P$ should also be small, and the value of K'$_I$ should be large. These values provide satisfactory system stability and avoid system oscillations. When the water level deviation EC is small, the value of K'$_D$ should be moderate, and when EC is large, the value of K'$_D$ is generally small. The control rules for K'$_P$, K'$_I$, and K'$_D$ are shown in Tables 1-3, respectively.

3) SIMULATION MODEL
The adjustment of the PID parameters is an important step in establishing the simulation model. The larger P is,
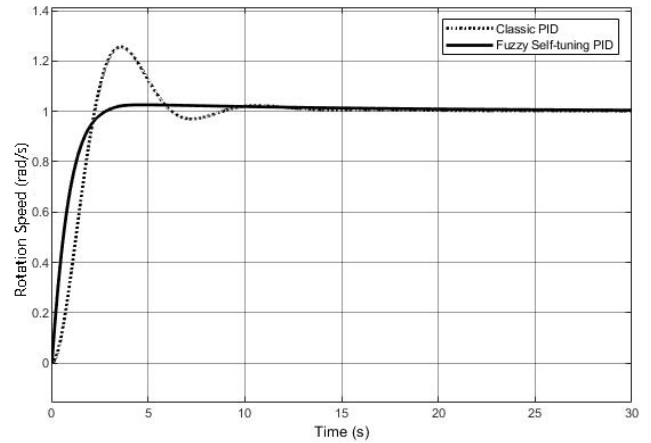

FIGURE 3. Classic PID and fuzzy parameter self-tuning PID simulation results. The dotted line in the figure represents the step response curve of the system after the classic PID control, and the solid line represents the step response curve of the system after the fuzzy PID control.

the stronger the setting, but the larger the error generated by the system. A small P system is more likely to oscillate. Moreover, the larger I is, the longer the system eliminates the error, and the smaller the I of the system is, the shorter the time, and the larger the system oscillation. The larger D is, the higher the system oscillation frequency, and a small-D system takes longer to reach a steady state.

A set of suitable PID parameters is determined as $K_P = 30$, $K_I = 3.5$, and $K_D = 30$, and the input is a unit step response. The structure of the PID control system in the data control acquisition system is determined, and the simulation graph is obtained through Simulink. The PID and autotuned PID are simultaneously input into the oscilloscope to compare the two methods. The simulation results are shown in Figure 3.

Figure 3 shows that the system divergence oscillation disappears after the system is controlled by the fuzzy PID and the classic PID. The stability is significantly improved, the overshoot is significantly reduced, the response time is greatly reduced, and the system is basically stable. However, the fuzzy PID is superior to the classic PID control. The system overshoot is reduced from 25% to 8%, the response time is reduced from 12 s to 5 s, the degree of overshoot is smaller, and the response speed is faster.

B. ANTI-WIND WAVE INTERFERENCE SIMULATION
1) RANDOM INTERFERENCE WAVE MODEL
In the offshore environment, there are often waves. When the underwater acquisition system moves to the offshore surface, it is susceptible to wave forces and shifts in conditions, which affect the function of the system. Therefore, to study the motion of the data acquisition controller in detail, we first establish a random wave interference model.

The wave curve of a wave is very complicated. To simplify wave motion and establish a mathematical wave model, the wave surface can be considered an infinite cosine wave superimposed [16]. These cosine waves have different amplitudes, different oscillation frequencies, different initial

phases and different directions of propagation.

$$U(t) = \sum_{i=1}^{\infty} Q_i \times \cos(\omega_i t + \varepsilon_i) \qquad (9)$$

$$Q_i = \sqrt{2 \times S(\omega_i) \times \Delta\omega} \qquad (10)$$

In the equations above, $U(t)$ is the amplitude of an ocean wave, and ε_i is a random variable that is evenly distributed between $[0, \pi]$ based on wave theory.

$S(\omega_i)$ is the spectral density function of the wave, and the P-M wave spectrum is the single parameter spectrum. These variables can be expressed as follows.

$$S(\omega i) = \frac{0.778}{\omega_i^5} \times \exp(\frac{-3.116}{\omega_i^4 \times H_{\frac{1}{3}}^2}) \qquad (11)$$

Due to variations in sea conditions, the parameters in the formula also change. The specific simulation frequency bands ωi and frequency increments $\Delta\omega$ for different sea conditions are shown in Table 4.

TABLE 4. Simulation frequency bands and frequency increments under different sea conditions.

Righteous wave height $H^2_{1/3}$/m	Simulation frequency band ω_i /(rad · s -1)	$\Delta\omega$/(rad · s -1)
<2. 5	0. 3 ~ 3. 0	0. 10
2. 5 ~ 5. 0	0. 24 ~ 2. 4	0.08
>5. 0	0. 08 ~ 1. 7	0.06

According to theoretical research, the energy of ocean waves is mainly concentrated in a certain frequency band [17]. Therefore, we only simulate the waves in this frequency range. The simulation results based on this approach are still representative, and the simulation precision requirements are met. In this paper, we use the frequency division method to determine the mean wave height $H^2_{1/3} = 2$ m, and ωi ranges from 0.3 to 3.0. Therefore, the ocean wave model can be simplified via the superposition of 28 sine functions with different frequencies.

$$U(t) = \sum_{i=1}^{28} Q_i \times \cos(\omega_i t + \varepsilon_i) \qquad (12)$$

Using MATLAB to calculate each Q_i value, $S(\omega_i)$, the spectrum of the random wave for the three-level sea state, is shown in Figure 4. The amplitude is shown in Figure 5.

2) ADDING A RANDOM WAVE INTERFERENCE MODEL TO THE SYSTEM

An interference model is added to the fuzzy control system simulation model, the PID system simulation model, and the fuzzy PID system simulation model, as shown in Figure 6.

In Figure 6, the response curves are based on the above simulation results. The system is disturbed by PID and fuzzy PID control. Although the system is basically stable at approximately 1 and the oscillation is eliminated, the system
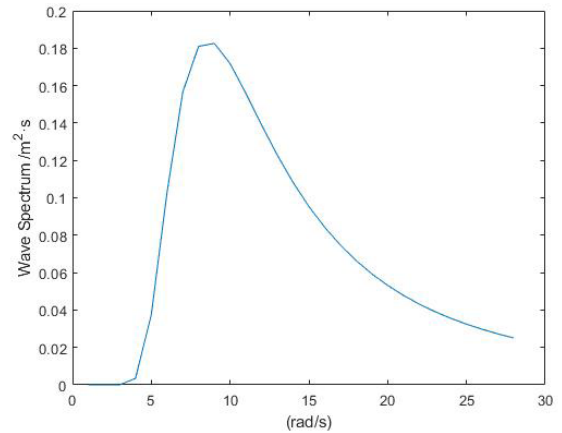

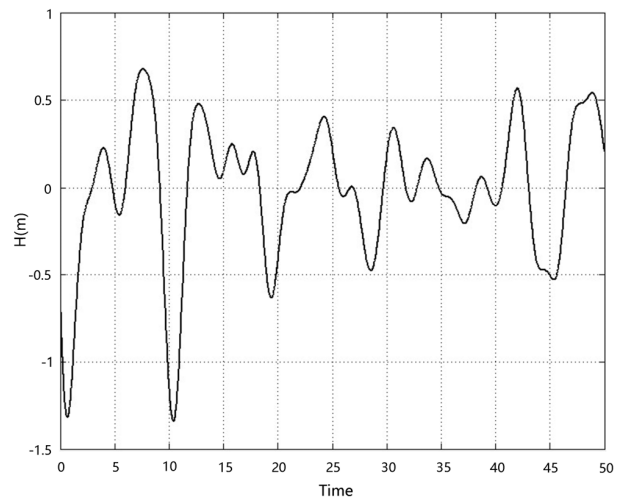**FIGURE 4.** Wave spectrum.

FIGURE 5. Wave amplitude.

overshoot significantly increases; although the above two methods have significant effects in controlling the automatic lifting and lowering of the underwater collecting system, the anti-interference ability of the random signal system needs to be improved.

3) DESIGN OF AN IMPULSE RESPONSE DIGITAL FILTER

The spectrum diagram of the wave in Figure. 5 shows that the frequency band of the wave that interferes with the movement of the underwater sealed cabin is mainly concentrated at approximately 1 Hz. Therefore, a lowpass filter is designed to reduce the interference of the sea waves. Considering the number of calculations and signal delay based on the same filtering index, we use a wireless impulse response (IIR) filter to remove the system interference associated with the ocean wave in real time [18].

The IIR filter is designed using the Digital Filter Design toolbox in the Simulink library. First, we select "Lowpass" as the filter type. Then, we select the infinite IIR filter for the "Design Method" option and the Chebyshev type I filter [19]. Next, we select "Minimum Order" as the "Filter Order" option (specify the automatic minimum order) and set the units to Hz in the "Frequency Specifications". The sampling
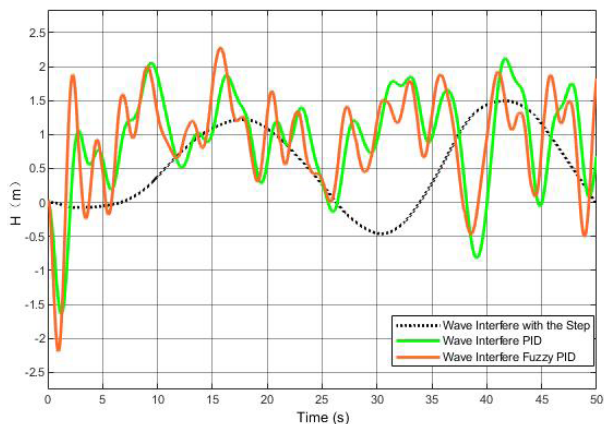
FIGURE 6. PID and fuzzy PID simulation results with sea wave interference. The dotted line represents the step response curve of the system after adding the wave interference model, the green line represents the step response curve of the system controlled by the PID after adding the wave interference model, and the red line represents the step response curve of the system controlled by the fuzzy PID after adding the wave interference model.
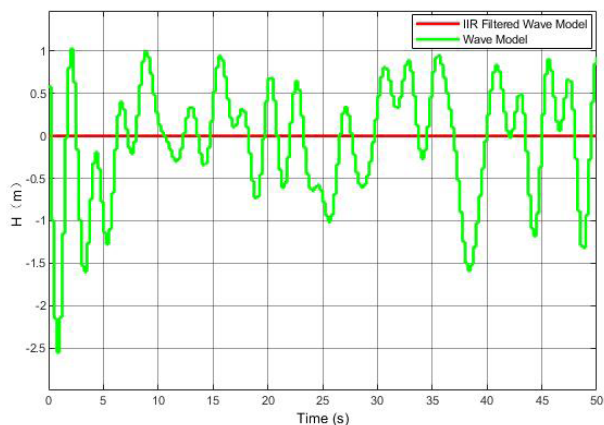

FIGURE 7. Wave filter simulation model. The green line represents the discretized wave model, and the red line represents the wave model after the IIR filter is applied.

frequency Fs = 2000, passband cutoff frequency Fpass = 0.047 Hz, and stopband cutoff frequency Fstop = 0.159 Hz. We set the units to db in the "Magnitude Specifications". The pass signal Apass = 0.2 in the passband, and the minimum attenuation Astop = 20 in the stopband. Finally, we click on "Design Filter" to automatically generate an IIR filter that meets the above requirements [20]. In addition, the characteristics of the amplitude-frequency response, phase frequency response, and impulse response of the filter can be obtained.

Because the digital filter is designed, the waveform of the ocean wave is first discretized. According to the sampling theorem, the sampling time is less than 1 s. Therefore, to ensure the accuracy of the ocean wave model, the sampling time for 28 cosine waves is set to 0.25 s. The simulation results are shown in Figure 7.

The simulation results show that the random interference model of the ocean wave maintains the original trend after discretization. The IIR lowpass digital filter largely eliminates the interference from waves, and the system can reach a stable state and meet the functional requirements of
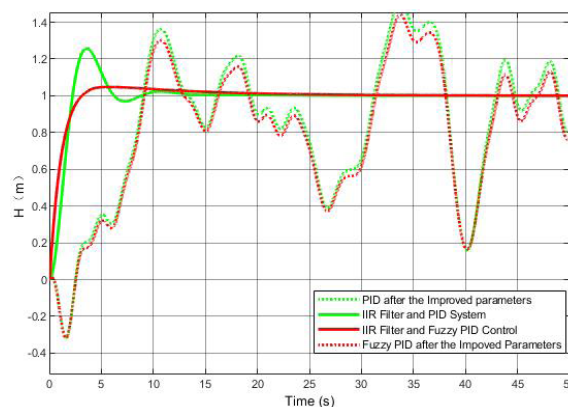

FIGURE 8. Simulation model for filtering sea wave interference using an IIR digital filter. The green solid line represents the step response curve of the IIR filter and the PID system after adding the wave interference model, and the red solid line represents the system step response curve of the IIR filter and the fuzzy PID control after adding the wave interference model. The green dotted line represents the step response curve of the system controlled by the PID after the improved parameters of the sea wave interference model are applied. The red dotted line represents the step response curve of the system controlled by the fuzzy PID after the improved parameters of the sea wave interference model are applied.

practical applications. The improved scheme is added to the system step response simulation model, and the simulation results are shown in Figure 8.

Overall, the IIR digital filter is effective. After wave interference is controlled by the classic PID and fuzzy PID, the system is stable, overshoot is reduced, the dynamic response time is short, and the dynamic and static performance of the system are significantly improved.

V. CONCLUSION

Based on simulation analysis, the proposed algorithm yielded a fast dynamic response, small overshoot and small error, with satisfactory dynamic performance. Therefore, this algorithm effectively minimized the fluctuations in the desired speed and achieved high precision to generate a smooth speed and good control effects. Compared with traditional buoys, which are limited to a certain fixed water level, the proposed approach is extremely dynamic. To collect water quality data at different water levels, multiple measuring devices are needed. Such an approach takes time and effort, and data acquisition is often limited and delayed. The proposed method does not limit the measurement range of the buoy. The measurement range can vary, and the underwater collection system can be automatically controlled. Water level sensors collect water quality data at different depths, and the system automatically adjusts the depth and position of monitoring according to the changes in the hydrological environment. The IIR digital filter can remove the effect of first-order ocean waves on the system considering the random interference of the ocean waves. Traditional buoys are influenced by forces generated by ocean waves, which can cause the stepping motor to not accurately reach the specified position. This issue can affect the measurement accuracy of the data acquisition system. The proposed method overcomes this issue,

wave interference is largely mitigated and the system is relatively stable. This method provides an important foundation for comprehensive analyses of the layered structure of water bodies and the stereoscopic distribution of water quality.

In this paper, some problems have not been well solved, and some new ideas have not been realized. Here, some possible future work is proposed. The data acquisition and control system designed in this paper is applied on the buoy, so the types of power supply are limited. The design of this paper does not consider low power consumption to reduce the energy consumption of the system. In future research, the system can be optimized, and the power management module can be designed to reduce the power consumption of the system. The system is limited to use only in offshore bays, but when the waves are much higher than level 3 in bad weather, the system can incorporate hall sensors to measure the output direction of lifting cables and reduce the impact of waves on the system by establishing a compensation model.

REFERENCES

[1] J. Trevathan, R. Johnstone, T. Chiffings, I. Atkinson, N. Bergmann, W. Read, S. Theiss, T. Myers, and T. Stevens, "SEMAT—The next generation of inexpensive marine environmental monitoring and measurement systems," *Sensors*, vol. 12, pp. 9711–9748, 2012.

[2] C. J. Pérez, M. A. Vega-Rodríguez, K. Reder, and M. Flörke, "A multi-objective artificial bee colony-based optimization approach to design water quality monitoring networks in river basins," *J. Cleaner Prod.*, vol. 166, pp. 579–589, Nov. 2017.

[3] D. Ashwini, M. Chidananda, and M. Z. Kurian, "Survey on multi sensor based air and water quality monitoring using IoT," *Indian J. Med. Res.*, vol. 17, no. 2, pp. 147–153, 2018.

[4] R. B. Wynn, V. A. I. Huvenne, T. P. L. Bas, B. J. Murton, D. P. Connelly, B. J. Bett, H. A. Ruhl, K. J. Morris, J. Peakall, D. R. Parsons, E. J. Sumner, and R. M. Dorrell, "Autonomous Underwater Vehicles (AUVs): Their past, present and future contributions to the advancement of marine geoscience," *Marine Geol.*, vol. 352, pp. 451–468, Jun. 2014.

[5] K. K. K. Ku, R. Bradbeer, P. Hodgson, K. Lam, and L. Yeung, "A low-cost, three-dimensional and real-time marine environment monitoring system, Databuoy with connection to the Internet," in *Proc. OCEANS MTS/IEEE Kobe Techno-Ocean*, Apr. 2008, pp. 1–5.

[6] D. Karimanzira, M. Jacobi, T. Pfuetzenreuter, M. Eichhorn, R. Taubert, and C. Ament, "First testing of an AUV mission planning and guidance system for water quality monitoring and fish behavior observation in net cage fish farming," *Inf. Process. Agricult.*, vol. 1, no. 2, pp. 131–140, Dec. 2014.

[7] A. H. A. H. Mohd, H. M. Muhammad, and R. M. S. B. Shah, "Mobile buoy for real time monitoring and assessment of water quality," in *Proc. IEEE Conf. Syst., Process Control (ICSPC)*, Dec. 2015, pp. 19–23.

[8] E. Anthony and B. Jeannette, "Development of a real-time water quality buoy for the fraser river estuary," in *Proc. OCEANS*, Oct. 2007, pp. 1–6.

[9] C. Peter, C. Bruce, E. B. James, and K. Roman, "Proactive management of estuarine algal blooms using an automated monitoring buoy coupled with an artificial neural network," *Environ. Model. Softw.*, vol. 61, pp. 393–409, Nov. 2014.

[10] G. Griffo, L. Piper, A. Lay-Ekuakille, and D. Pellicanò, "Design of buoy station for marine pollutant detection," *Measurement*, vol. 47, pp. 1024–1029, Jan. 2014.

[11] M. P. Chavarría and E. E. Zamora, "Development of a data acquisition system for an oceanographic buor," *J. Appl. Res. Technol.*, vol. 7, no. 2, pp. 193–201, Aug. 2009.

[12] J. Sorribas, A. Tudela, A. Castellon, O. Chic, Z. Garcia, J. Prades, and D. Montero, "An oceanographic data acquisition system (ODAS) for Ethernet LANs for spanish research vessels," in *Proc. IEEE Ocean. Eng. Soc., OCEANS. Conf.*, vol. 1, Sep. 1998, pp. 93–97.

[13] W. Q. Xu and J. H. Yan, "Derivation of transmission function model of two-phase hybrid stepping motor," *Space Electron. Technol.*, vol. 3, pp. 50–53, Mar. 2011.

[14] F. C. Lin and S. M. Yang, "Two-phase linear stepping motor control with three-leg VSI and on-line dead-time compensation," *J. Chin. Inst. Eng.*, vol. 28, no. 6, pp. 967–975, 2005.

[15] S. Jaszczak and J. Kołodziejczyk, "A method of fast application of the fuzzy PID algorithm using industrial control device," in *Proc. Int. Conf. Artif. Intell. Soft Comput.*, 2012, pp. 237–246.

[16] L. I. Zun-Hua, J. F. Xing, J. Xue, and G. L. Hou, "Real-time simulation on the movement of the underwater aircraft in ocean waves based on Simulink," *Ship Eng.*, pp. 44–48, 2007.

[17] H. L. Chen, L. I. Ai Jun, and H. Y. Jia, "Real-time simulation and spectral analysis of sea wave signal," *Electr. Mach. Control*, vol. 11, no. 1, p. 93, 2007.

[18] D. J. Jung and K. Chang, "Low-pass filter design through the accurate analysis of electromagnetic-bandgap geometry on the ground plane," *IEEE Trans. Microw. Theory Techn.*, vol. 57, no. 7, pp. 1798–1805, Jul. 2009.

[19] Y. H. Wang, X. Bian, and X. Shi, "A simulation of wave disturbance and filter design," *Comput. Simul.*, vol. 4, pp. 318–321, Apr. 2007.

[20] Q. H. Shi, "Design and simulation of IIR digital filter based on MATLAB/FDATOOL," *Sci. Mosaic*, pp. 56–58, 2010.

YAOGUANG WEI received the Ph.D. degree from the University of Science and Technology Beijing, in 2005. He is currently an Associate Professor with the College of Information and Electrical Engineering, China Agricultural University. His current research interests include underwater robot and intelligent agriculture.

YINGHAO WU is currently pursuing the master's degree in computer technology with the Department of Information and Electrical Engineering, China Agricultural University, Beijing, China. His main research direction is underwater robot positioning and navigation.

XU ZHANG is currently pursuing the master's degree with the Department of Information and Electrical Engineering, China Agricultural University, Beijing, China. Her main research direction is stereo monitoring of the seawater environment.

JIAHUI REN is currently pursuing the master's degree with the Department of Information and Electrical Engineering, China Agricultural University, Beijing, China. His main research direction is motion control of underwater robots.
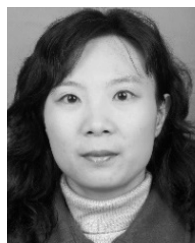
DONG AN received the Ph.D. degree from the Institute of Semiconductors, Chinese Academy of Sciences, in 2005. She is currently a Professor with the College of Information and Electrical Engineering, China Agricultural University. Her current research interests include image processing, underwater robots, and intelligent agriculture.

• • •